MRS Communications (2018), *8*, 903–910
© Materials Research Society, 2018
doi:10.1557/mrc.2018.100

MRS Communications

Research Letter

Natural eggshell membranes exhibiting programmable shape recovery characteristics

Chang Liu, Shenyang National Laboratory for Materials Science, Institute of Metal Research, Chinese Academy of Sciences, Shenyang, Liaoning 110016, China; Department of Chemistry, Northeastern University, Shenyang, Liaoning 110004, China
Chen Liu, Shenyang National Laboratory for Materials Science, Institute of Metal Research, Chinese Academy of Sciences, Shenyang, Liaoning 110016, China
Qian Li, Department of Chemistry, Northeastern University, Shenyang, Liaoning 110004, China
Miao Song, Pacific Northwest National Laboratory, Richland, WA 99352, USA
Dun Niu, Department of Chemistry, Northeastern University, Shenyang, Liaoning 110004, China
Mingming Ma, Department of Chemistry, University of Science and Technology of China, Hefei, Anhui, 230026, China
Xing Zhang, Shenyang National Laboratory for Materials Science, Institute of Metal Research, Chinese Academy of Sciences, Shenyang, Liaoning 110016, China; School of Materials Sciences and Engineering, University of Science and Technology of China, Hefei, Anhui, 230026, China

Address all correspondence to Xing Zhang, Dun Niu, Mingming Ma at **xingzhang@imr.ac.cn**, **niudun666@hotmail.com**, **mma@ustc.edu.cn**

(Received 17 April 2018; accepted 23 May 2018)

Abstract

In this study, a novel shape memory polymer (SMP), eggshell membrane (ESM), with macroscopic mesh structures and microscopic cross-linked protein fibers, has shown water-stimulated shape recovery characteristics. Our results show that the collagen triple-helical molecular chains and disulfide-rich motifs in the ESM function as net-points retaining essential structures during deformation, while hydrogen bonds play a key role as switch units for shape recovery through water stimulation. We also demonstrate that programmable shape recovery characteristics of ESM can be obtained by modulating the number of net-points. This study may inspire the design of new programmable SMPs.

Introduction

Shape memory polymers (SMPs) are stimulus-responsive materials that have the ability to recover their original shapes after being deformed into temporary shapes by applying specific external stimuli, such as heat,[1,2] light,[3,4] alternative magnetic field,[5] electricity,[6,7] or solvent/water.[8–10] Among them, water-stimulated SMPs are able to recover their original shapes from temporary deformation through interaction with water. Synthetic water-responsive SMPs including poly(ethylene glycol) hydrogels,[9] polypyrrole composite films,[10] and poly(vinyl alcohol)[11] have been developed for water-driven actuation and biomedical applications. Natural water-responsive SMPs produced by biologic systems, including animal hairs,[12] peacock's tail covert feathers,[13] caddisfly silk,[14] and spider draglines[15] have also been recently reported. Previous studies mainly focused on the illustration of excellent mechanical adaptivity and shape recovery characteristics of these natural water-responsive SMPs in relation to their unique microstructures and chemical compositions (net-points and switch units). However, modification of these natural SMPs for programmable shape recovery characteristics has rarely been investigated.

The natural eggshell membrane (ESM) is composed of double-layer meshwork of collagen, keratin, elastin, etc.[16,17] The relatively high content of cysteine results in a large number of disulfide bond crosslinks among the protein constituents, leading to the insolubility of ESM in water. Disulfide bonds are commonly considered as net-points of SMPs, which are not sensitive to certain external stimuli such as water.[18] Moreover, the inter-chain H-bonds form among the protein constituents of the ESM, which can serve as switch units for the shape recovery. In this study, the chemical compositions, microstructures, and mechanical properties of chicken ESM samples are investigated to illustrate the underlying mechanisms for the shape recovery.

Materials and methods

Raw materials

Chicken eggs were procured from local stores. The ESM samples were carefully separated from their shells by peeling-off and rinsed with deionized water. ESM samples with the thickness ~70–80 μm were used for further experiments. All chemical reagents (the analytical grade) used in the experiments were bought from Sinopharm Chemical Reagent Co., Ltd. (Beijing, China). The ESM samples completely hydrated in water were named as "wet ESM", whereas those completely dried in air were named as "dry ESM".

Morphology and composition analyses

The chicken ESM samples were dehydrated in a series of ethanol–water solutions at different ethanol volumetric concentrations (50%, 60%, 70%, 80%, 90%, 100%) for 15 min each

https://doi.org/10.1557/mrc.2018.100 Published online by Cambridge University Press

time, except three times for pure ethanol (100%), which were then used for microstructure and element analysis using a field emission scanning electron microscope (SEM, Zeiss Supra 35, Germany) and the energy-dispersive spectroscopy (EDS, Oxford INCAX 7582, UK). A total of 100 fibers were randomly chosen from five SEM images (20 fibers per image) for the measurement of fiber width. A Tecnai G2 F20 transmission electron microscope (TEM, Tecnai G2 F20, FEI, Hillsboro, USA), equipped with a high-angle annular-dark-field (HAADF) detector and an x-ray EDS system, was used for bright-field imaging at 200 kV, HAADF scanning TEM imaging, and element composition analysis. X-ray diffraction (XRD) was performed for ESM samples using an x-ray diffractometer (Rigaku D/max 2400, Tokyo, Japan) operated at 40 kV with Cu $K_{\alpha 1}$ of 1.5418 Å. The scanning range 2θ was 10–40° with a stepwise of 0.04°. Attenuated total reflection-Fourier transform infrared (ATR-FTIR) spectra (wavenumber 600–4000/cm) were conducted using a FTIR spectrometer (Tensor 27, Bruker, Germany).

Effect of stimulation medium on shape recovery

Cleaned ESM samples were cut into rectangular shapes ~40 mm (length) × 6 mm (width). Wet ESM samples were rotated (diameter ~4.5 mm) to form helical shapes around a plastic rod. Chicken ESM samples were also folded to form zig-zag shapes with an Allen wrench (side size 3/8 inch). The dried samples were immersed in deionized water to record the shape recovery process ($n = 5$). The dried helical-shape and zig-zag-shape ESM samples were immersed in three types of media, deionized water, 70% (v/v) ethanol (with water), pure ethanol, respectively, to study the effect of medium on the recovery processes ($n = 5$). Water-responsive shape recovery of goose and quail ESM samples was also investigated. In this study, all experiments were conducted at room temperature unless otherwise noted. Videos and screenshots were taken by iPad Air 2 iSight camera with a new eight-million-pixel sensor (Apple Inc., Cupertino, California, USA).

Effect of protein thiolation and denaturation on shape recovery

Ammonium hydroxide (~25–28%) was mixed to the 10% (v/v) thioglycolic acid solution to obtain an ammonium thioglycolate solution (pH ~8–9). The chicken ESM samples were soaked in the ammonium thioglycolate solution for 8 h, and then rinsed with the ultrapure water (A 10, Millipore, Billerica, MA, USA) thrice. Disulfide and thiol functional groups for original ESM and thiolated ESM samples (named as "thiolated-ESM") under wet and dry conditions were characterized using a Raman spectrometer (XploRA plus, Horiba scientific, Tokyo, Japan). Calorimetric measurement was performed to obtain the denaturation temperature for original ESM samples using a thermal analysis instrument (TGA/DSC 1, Mettler Toledo, Switzerland). ESM samples were soaked in hot water (70 °C) for an hour for protein denaturation (named as "denatured-ESM"). Original chicken ESM, thiolated-ESM, and denatured-ESM samples were rotated on a plastic rod (diameter ~4.5 mm) to form helical shapes, which were further dried in air for 24 h to fix the shapes. These dried samples were then immersed in deionized water to record the recovery process using iPad Air 2 ($n = 5$).

Mechanical tests

The uniaxial tension test for the chicken ESM samples in 20 mm (length) × 4 mm (width) were conducted by a TA Electroforce ELF 3200 system (Eden Prairie, MN, USA). The crosshead speed of 0.01 mm/s and gauge length of 10 mm were set for tension tests. All samples were immersed in three types of media [deionized water, 70% (v/v) ethanol, pure ethanol] during the tests. Five duplicates of each sample were tested. The loading force and displacement were recorded in each test, and divided by the cross-sectional area and gauge length of the sample, respectively, to obtain stress and strain values. The elastic modulus of each sample was determined as the slope of the linear region in the stress–strain curve. Stress relaxation behavior under uniaxial tension was evaluated with an initial strain of 1% for dry ESM samples, and 1% or 10% initial strain for wet ESM samples ($n = 3$). Moreover, dynamic mechanic analyses (DMA) of ESM samples were performed under the tensile mode by applying a sinusoidal wave with a maximum strain of 30% from 1 to 5 Hz ($n = 5$).

Adhesion trials

Two ESM samples were separately attached to two loading plates by adhesive tapes, and were then adhered to each other with an effective contact area of ~5 cm^2. Two, three, or four ESM layers were adhered to each other following the above method, which were further dried in air for 24 h. Adhesion between ESM samples was demonstrated by hanging different weights (100 or 200 g). The actual adhesion force between the ESM layers was measured by a TA Electroforce ELF 3200 system, which was further used to calculate the interface bonding strength by dividing the effective contact area ($n = 3$). "ESM" and "SEM" symbols were written on two rectangular ESM samples [18 mm (length) × 10 mm (width)] by NO.2 pencil, which were further adhered to each other by drying in air for 24 h. The dried samples were then immersed in deionized water for separation to show the symbols ($n = 3$).

Effect of glutaraldehyde crosslinking on shape recovery

Wet ESM samples were rotated (diameter ~4.5 mm) to form helical shapes around plastic rods, which were then placed above 3 mL 25 wt.% glutaraldehyde (GA) solutions in the 15 mL centrifuge tubes. ESM samples were crosslinked with GA vapor for 15 min, 30 min, 1 h, and 2 h, respectively. The GA crosslinked ESM samples were named as "GA-ESM". GA-ESM samples were immersed in deionized water in the hydration process. The wet GA-ESM samples were then placed

https://doi.org/10.1557/mrc.2018.100 Published online by Cambridge University Press

in air to record the shape recovery to helical shapes by a dehydration process at room temperature ($n = 3$).

Statistical analysis

All data were expressed as mean ± standard deviation (SD). Statistical significance was analyzed by one-way analysis of variance with the Tukey post hoc testing. The p value <0.05 was considered to be statistically significant.

Results and discussion

Water-stimulated shape memory effect

Figure 1 shows that dry zig-zag-shape and helical-shape chicken ESM samples can fully recover their original shapes (rectangular strips) in approximate 2 and 4 s, respectively, after immersed in water at room temperature. Helical-shape goose and quail ESM samples can also recover their original shapes in 3 and 6 s, respectively (Fig. S1). When immersed in a 70% (v/v) ethanol–water solution, the recovery time was about 4 and 7 s for zig-zag-shape and helical-shape chicken ESM samples, respectively, much longer than those in water (Fig. S2). Moreover, these samples cannot return to their original shapes when immersed in pure ethanol. These results suggest that the shape memory effect of the ESM is mediated by water.

Chemical compositions and microstructures of ESM

The chemical compositions of SMPs play an important role in the shape memory effects. ESM samples are composed of highly crosslinked protein fiber networks. Figures 2(a) and 2(b) show that the inner and outer layers of the ESM consist of a network of protein fibers with an average diameter of 0.96 ± 0.26 and 2.01 ± 0.69 μm, respectively. These fibers comprising of core–mantle complex structures [Fig. 2(d)] form trunks and branches (dendritic structures), consistent with the TEM results [Fig. 2(e)]. The dendritic structures are shown in Figs. 2(f) and 2(g). Previous studies indicate that the major ESM fibers are composed of collagen-rich cores including type I, V, and X collagens and glycoprotein-rich mantles with desmosine and isodesmosine crosslinks.[19] Moreover, a previous study shows that the outer membrane consists of keratin–mucin complex, whereas the inner membrane contains finer keratin and mucin fibers.[20] The EDS result [Fig. 2(c)] indicates the compositions of C, S, O, Ca elements, while EDS mapping [Fig. 2(i)] of an ESM fiber from TEM further shows uniform distribution of C, S, O elements. Identification of Ca elements in the ESM sample corresponds to the existence of a small amount of $CaCO_3$ granules in the outer membrane of ESM.[21] Identification of S elements [Fig. 2(i)] corresponds well with the cysteine-rich composition with disulfide crosslinks (i.e., keratin and CREMP protein), consistent with the previous findings.[22]

Effect of thiolation and denaturation on shape recovery

A broad peak is present on the XRD pattern of the wet ESM sample [Fig. 3(a)], indicating disruption of microscopically

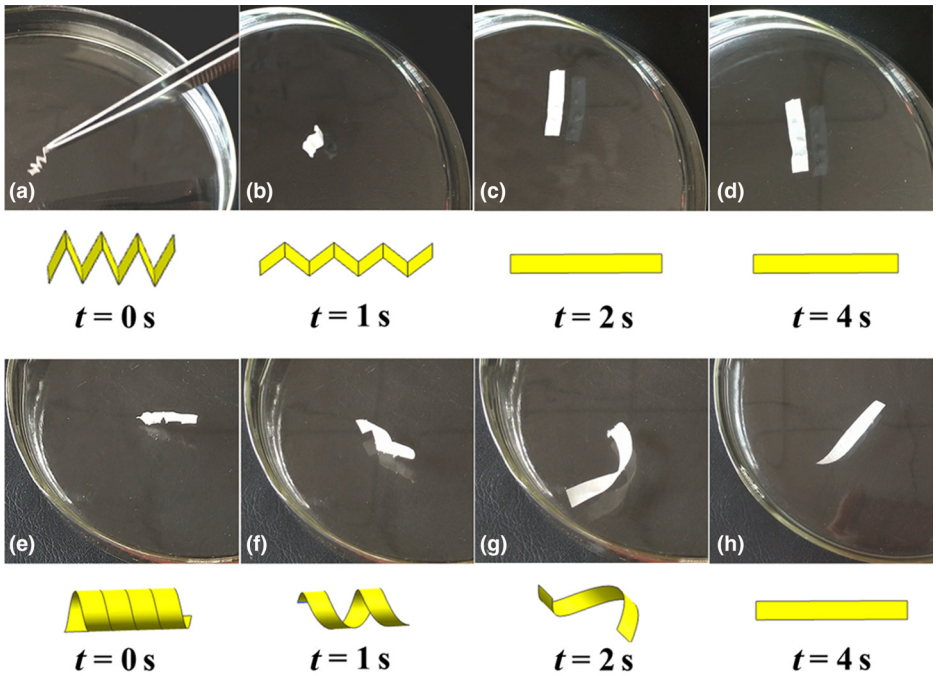


Figure 1. The shape recovery of dry chicken ESM samples by hydration in water at room temperature. (a–d) The shape recovery process for a zig-zag-shape ESM sample. (e–h) The shape recovery process for a helical-shape ESM sample.

https://doi.org/10.1557/mrc.2018.100 Published online by Cambridge University Press

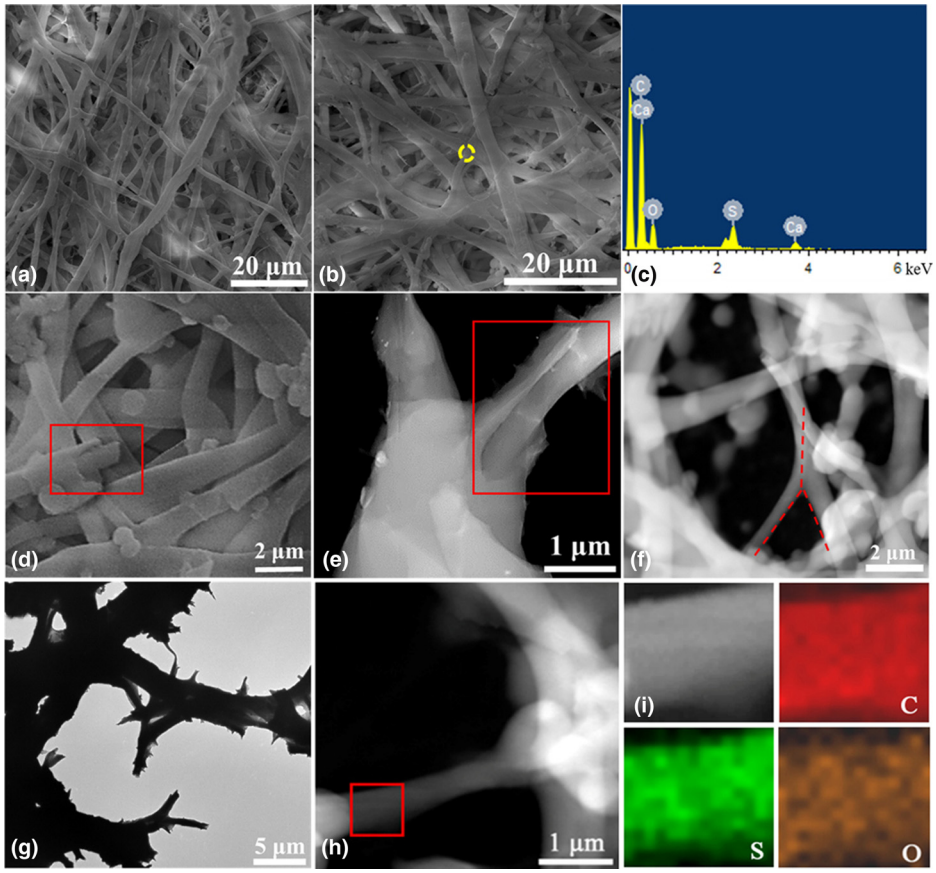


Figure 2. SEM micrographs of the protein fibers in (a) the inner layer membrane and (b) the outer layer membrane, as well as (c) the corresponding EDS result from the yellow dash circle area in (b). SEM and TEM images of protein fibers with (d, e) the core–mantle structures of ESM fibers (indicated by the red rectangles) and (f, g) dendritic structures (indicated by red dash lines in (f)). (i) The corresponding EDS mapping for C, S, and O elements from the red square area in (h).

ordered arrangement of polypeptide chains by hydration. After dehydration in air for 2 hours, there is no obvious change of the XRD pattern. However, a diffraction peak at 21.4° is present in the XRD patterns after dehydration for 9, 16, and 24 h, which can be ascribed to the sequence and conformations of amino acids from ESM fibers.[23] Moreover, two other diffraction peaks around 23.8° and 29.4° are shown in the XRD patterns of ESM samples after dehydration for 24 h, likely corresponding to the crystalline units of collagens from ESM fibers [Fig. 3(a)].[24] This is likely due to the formation of intermolecular H-bonds during dehydration, which facilitates the organized stack of collagen polypeptide chains and further shapes aggregation structures of protein fibers, resulting in a crystalline property.[24] Comparing the ATR-FTIR spectrum from the dry sample to that from the wet sample [Fig. 3(b)], vibration peaks for C = O stretching (amide band I) and NH bending (amide band II and III) shift to higher wavenumbers from 1630 to 1638, 1523 to 1545, and 1234 to 1238/cm, respectively. These results indicate that H-bonds form between these residues and water molecules during the hydration process, consistent with the previous findings.[25] The broad absorption band around 3400/cm present on the ATR-FTIR curve for the wet ESM sample corresponds to free water. On the other hand, there is a small peak present in the spectrum for the dry ESM sample, corresponding to the hydroxyl group and the remaining H_2O in the sample. These results suggest that water molecules including the free water and the bound water can diffuse into the fibrous networks of dry ESM during the hydration process, and act as plasticizers (switch units) resulting in shape recovery.

Disulfide bonds (S–S) play a significant role as net-points in the water-responsive shape memory effect for SMPs. Thioglycolate reduction can be used to produce thiol (–SH) groups on the ESM surface by S–S bond cleavage.[26] Raman spectra of the original ESM and the thiolated-ESM samples are shown in Fig. 3(c). The peak around 505/cm in the Raman spectrum corresponds to the stretching mode of the S–S bond, while the stretching of the S–H bond is present around 2569/cm. The S–S bonds are present in both dry and wet ESM samples, suggesting that the disulfide bonds serve as dominating net-points insensitive to external water environment. However, this characteristic S–S bond signature

https://doi.org/10.1557/mrc.2018.100 Published online by Cambridge University Press

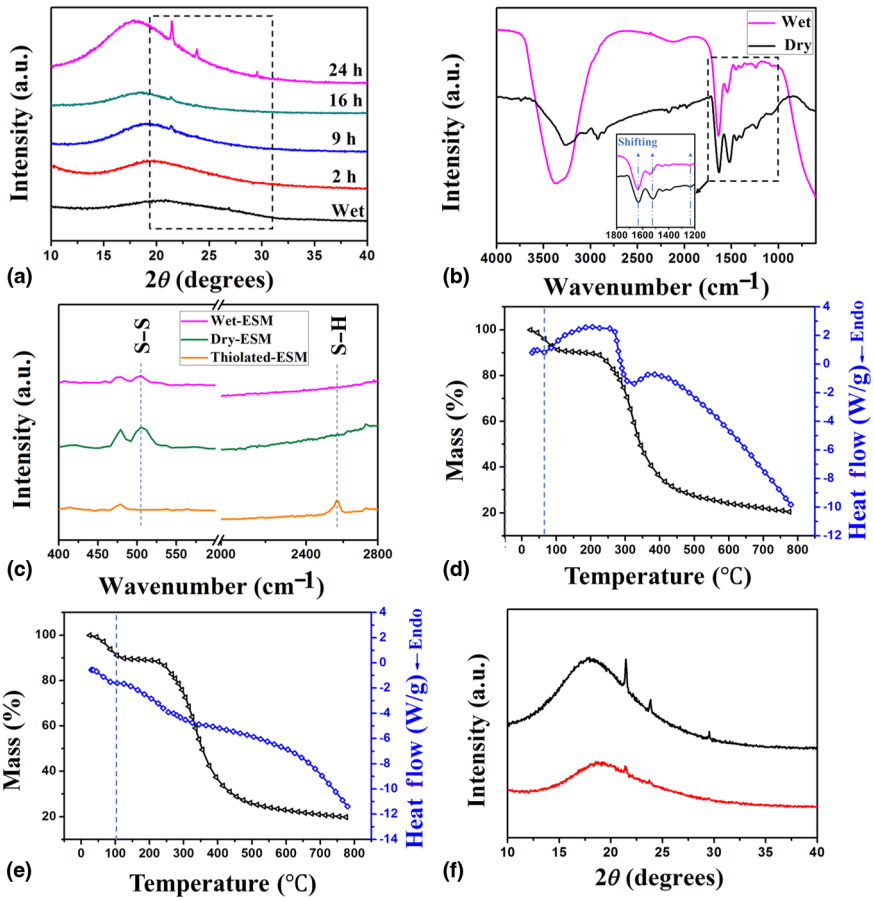


Figure 3. (a) XRD patterns of the wet-ESM sample and samples after dehydration for 2, 9, 16, 24 h. (b) ATR-FTIR spectra of dry and wet ESM samples and the shifting of the absorption peaks comparing the dry and wet ESM samples (inset). (c) Raman spectra of original ESM and thiolated-ESM (magnified intensity (10×) were plotted to show the peaks). (d, e) TG (black) and DSC (blue) curves of original ESM (d) and denatured-ESM samples (e). (f) XRD patterns of dry original ESM (black) and denatured-ESM (red) samples.

disappears by thioglycolate reduction, while the S–H bond signature appears for the thiolated-ESM sample. When helical-shape thiolated-ESM samples were immersed in water, the recovery was much slower (~28 s) compared with original ESMs (Fig. S3), likely due to the decrease of the total number of net-points by partial thioglycolate reduction.

An endothermic peak around 60–65 °C is present in the differential scanning calorimetry (DSC) curve for the original ESM sample [Fig. 3(d)], which is likely attributed to collagen denaturation and water evaporation. On the other hand, there is only a shoulder peak around 100 °C for the denatured-ESM sample [Fig. 3(e)], corresponding to water evaporation indicated by the weight loss in the TG curve. In addition, the XRD result [Fig. 3(f)] of the denatured-ESM sample shows relatively lower crystallinity compared with the original ESM sample [Fig. 3(a)], probably due to the disruption of polypeptide chain structures. These dry denatured-ESM samples cannot recover to the initial helical shapes by hydration. It is worth noting that there is an obvious disruption of fibrous structures for denatured-ESM samples [Fig. S4(A)], while thiolated-ESM samples retain their original fibrous structures of ESM [Fig. S4(B)] and show shape recovery. The above results suggest that the shape recovery characteristics can be programmed by the modulation of net-points and switch units of ESM samples.

Mechanical properties

Mechanical behavior of chicken ESM samples under different conditions was studied. Representative stress–strain curves of the ESM tested in water, 70% ethanol-water solution (v/v), pure ethanol, and in the dry status are shown in Fig. 4(a). Elastic moduli of ESM samples in water, 70% ethanol–water solution (v/v), pure ethanol, and in the dry status are 3.51 ± 0.48, 4.65 ± 0.63, 11.34 ± 1.41, and 227.96 ± 8.54 MPa, respectively [Fig. 4(b)], in the order from low to high. Significant decrease of elastic moduli of ESM samples after hydration suggests weakening of inter-chain H-bonds among protein fibers by water interaction. Compared with ethanol

https://doi.org/10.1557/mrc.2018.100 Published online by Cambridge University Press

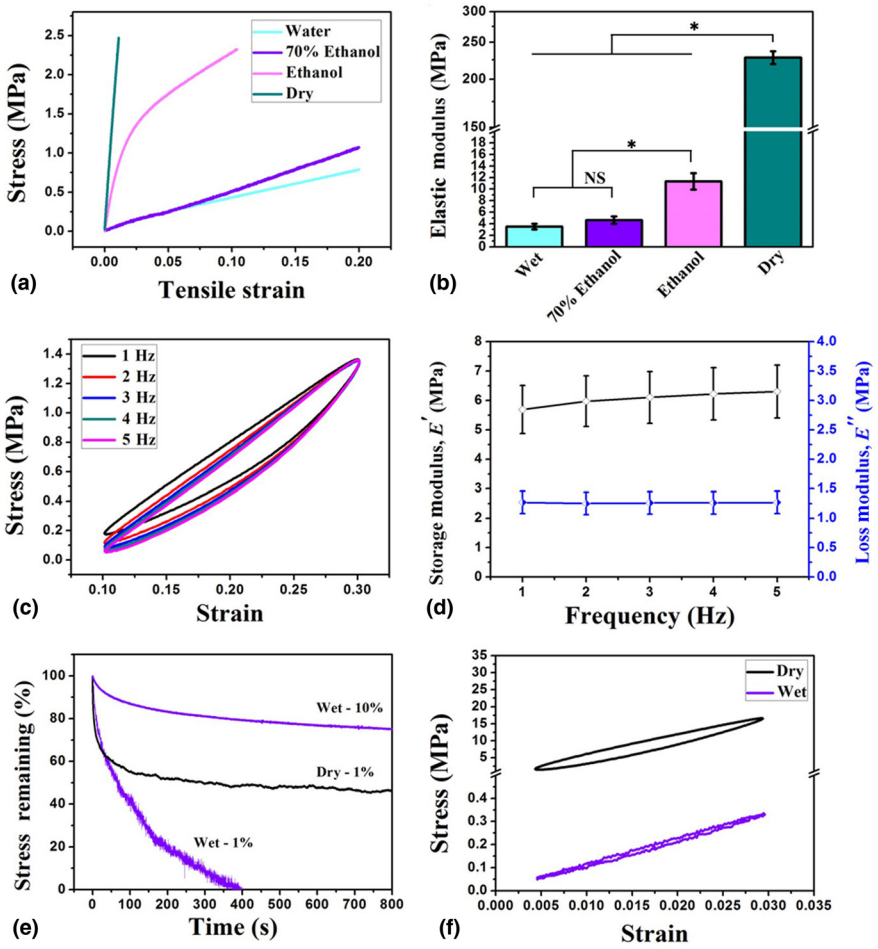


Figure 4. (a) Representative stress–strain curves and (b) calculated elastic moduli of the ESM samples tested in water, 70% ethanol (v/v), pure ethanol, and in the dry status. "NS" means no significant difference and $*p < 0.001$ indicates significant difference among groups (c). Stress–strain curves and (d) variations of storage modulus E' and loss modulus E'' of ESM samples in water under DMA tests with a strain rate from 10 to 30% and a frequency from 1 to 5 Hz. (e) Stress relaxation for ESM samples when immersed in water (wet status) and dried in air (dry status). (f) Stress–strain curves of wet and dry ESM samples under DMA tests with a strain rate from 0.5 to 3% and a frequency of 1 Hz.

molecules, water molecules with higher polarity are more likely to form H-bonds with functional groups (i.e., amide and hydroxyl) on the surfaces of ESM fibers. At a low stress level, molecular rearrangement can occur through uncoiling or straightening with the rearrangement of protein molecules in the aqueous environment.[27] Disruption of H-bonds in ESM results in the swelling of ESM samples and enhances flexibility of polypeptide chains, leading to the recovery to the initial shape.

The DMA tests were further used to investigate the shape recovery characteristics under cyclical tensile loading at 1–5 Hz. Typical stress–strain hysteresis loops with a strain range of 10–30% were observed for the ESM samples immersed in water [Fig. 4(c)], indicating the viscoelastic behavior of ESM similar to other biopolymers (e.g., spider silk). The hysteresis loop with a strain range of 10–30% tends to become identical after the 1 Hz hysteretic cycle and with no significant variation for further hysteretic cycles (from 2 to 5 Hz), revealing the efficient energy dissipation capacity of ESM samples and structural integrity during load and unload cycles. As the frequency increases from 1 to 5 Hz, the storage modulus E' slightly increases from 5.69 ± 0.82 to 6.30 ± 0.90 MPa, and the loss modulus E'' remains essentially constant [Fig. 4(d)], indicating a constant hysteresis energy dissipation.

For stress relaxation, the remaining stress decreases to 65% from an initial strain rate of 1% in about 50 s for both dry and wet status. The remaining stress then slowly decreases until reaching a plateau about 50% in 100 s for the dry status, while that for the wet status decreases to zero at a sharp rate. On the other hand, the remaining stress slightly decreases to 75% even until 800 s for wet ESM samples when the initial strain is 10% [Fig. 4(e)]. Moreover, wet ESM samples show significantly lower stress and lower energy dissipation than dry ones at the same tensile strain, according to the hysteresis

https://doi.org/10.1557/mrc.2018.100 Published online by Cambridge University Press

loops [Fig. 4(f)]. These results again demonstrate that water molecules play as effective plasticizers in structural rearrangement for ESM fibers.

Adhesion trials

Wet ESM samples can adhere to each other after drying, which are able to support a hanging weight of 100 g [Fig. S5(A)], likely due to the interfacial bonding from H-bonding between protein fibers. The adhesion force between two dry ESM samples was measured to be 4.02 ± 1.88 N (bonding strength ~8.04 ± 3.76 kPa). When immersed in water, the two samples separate from each other due to the disruption of H-bonds among protein fibers by water [Fig. S5(B)]. Moreover, the adhesion strength increases from 8.04 ± 3.76 kPa at two layers to 83.88 ± 29.96 kPa at three layers. However, the adhesion strength decreases to 22.54 ± 9.28 kPa at four layers, likely due to loosed contact among ESM layers [Fig. S5(C)]. The remarkable adhesion effect from ESM samples may be further used for other applications, i.e., reusable adhesive. "ESM" and "SME" symbols were written on dry ESM samples by a pencil [Fig. S5(D)]. The samples were then hydrated, and adhered to each other after drying to hide the symbols [Fig. S5(E)]. When exposed to water, the ESM samples separate again and the symbols are shown [Fig. S5(F)]. The symbols become clear with the evaporation of water [Fig. S5(G)], indicating the integrate structures of ESM samples after bonding and de-bonding processes. Thus, ESM samples with shape memory characteristics may have potential advantages in reusable adhesive.

Effect of GA crosslinking on shape recovery

Dry ESM samples with temporary shapes (helical/zigzag) show efficient shape recovery to initial shapes by hydration. However, the hydrated ESM samples are not able to form the helical/zig-zag shapes by dehydration in air without additional physical support, likely due to low stiffness of these samples. GA is the most commonly used and effective crosslinker, which has been used for crosslinking of protein fibers in ESM samples to increase the stiffness and enhance the stability.[17] As shown in Figs. S6(A)–6(D), the stiffness of GA-ESM samples increases with the increase of crosslinking time (increase of the total number of net-points by GA crosslinking). It is worth noting that wet GA-ESM samples with GA crosslinking for 1 h can gradually return to helical shapes by dehydration in air for 12 min [Figs. S6(E)–6(H)]. Thus, addition of new net-points by chemical crosslinking to a certain degree can significantly improve the shape recovery characteristics of ESM samples. These results again confirm that the shape recovery characteristics can be programmed by the modulation of the total number of net-points.

Water-stimulated shape recovery characteristics mechanism for ESMs

Water-induced shape memory effect for ESM evidently correlates to their hierarchical structures and heterogenic chemical compositions. For example, chicken ESM samples consist of inner and outer protein fibrous membranes [Fig. S7(A)]. A previous study reveals that fiber cores [Fig. S7(B)] from the outer membrane predominantly comprise type I collagen, whereas those from the inner membrane mainly consist of types I and V collagens.[28] The triple-helical molecular chains are mainly connected by strong interchain H-bonds and act as net-points, which support the stability and mechanics of collagen fibers. In the initial stage of deformation (strain ~3–4%), collagen fibers extend by the molecular rearrangement through uncoiling or straightening the triple helical structures of collagens in water environment.[29] Thus, water-induced shape recovery from a small deformation corresponds to the reconfiguration of collagen fibers without covalent bond breaking [Figs. S7 (C) and 7(D)]. Disulfide bonds (S–S) play a significant role as net-points in the water-responsive shape memory effect for SMPs. When thioglycolate reduction was used to produce thiol (–SH) groups on the ESM surface by S–S bond cleavage, the recovery was much slower than original ESMs, likely due to the decrease of the total number of net-points by partial thioglycolate reduction [Fig. S7(E)]. However, denatured-ESM samples cannot recover to original shapes when immersed in water, possibly because that the protein denaturation results in the rupture of inter-chain H-bonds and rearrangement of collagen triple helices into random chain configuration [Fig. S7 (F)].[30] Water molecules can quickly diffuse into the porous structures of ESM samples (porosity ~30–50% for chicken ESM) and act as plasticizer agents for ESM fibers [Figs. S8 (A) and 8(B)]. The mantle parts of ESMs mainly comprise glycoproteins.[19] There are abundant C = O and NH functional groups on the mantle surfaces that tend to form H-bonds serving as switch units [Figs. S8(C) and 8(D)]. When exposed to water, debonding of original innate H-bonds among protein fibers (especially those from mantle surfaces) lead to fast recovery to the original shape from dry status.

Conclusions

The ESM, consisting of porous protein fibrous membranes, has shown water-induced shape recovery characteristics. The hierarchical structures including macro-, micro-, and nano-structures and heterogenic compositions play important roles in the shape recovery of ESM samples. At the macroscopic level, the porous structures of ESM samples allow fast diffusion of water molecules that act as plasticizer agents for ESM fibers. At the microscopic level, the chicken ESM fibers are mainly composed of collagen-rich cores and glycoprotein-rich mantles. H-bonds especially those in glycoprotein-rich mantles play a key role as switch units, which can be disrupted by water molecules in the hydration process, leading to the shape recovery from the dry status to the wet status. At the nano-size level, collagen triple-helical molecular chains and disulfide-rich motifs in ESM samples function as net-points, which stabilize essential structures for temporary deformation during the dehydration process. We also demonstrate that the shape recovery characteristics of ESM samples can be programmed by modulating the number of net-points (i.e., existing

https://doi.org/10.1557/mrc.2018.100 Published online by Cambridge University Press

disulfide bonds or new GA crosslinking). Moreover, multiple ESM layers can be assembled and dissembled by dehydration and rehydration processes, which may be further used for reusable adhesives. Therefore, natural ESMs with water-induced shape recovery characteristics may inspire the design of novel programmable SMPs for many applications.

Supplementary material

The supplementary material for this article can be found at https://doi.org/10.1557/mrc.2018.100

Acknowledgments

This work was supported by the National Natural Science Foundation of China (31670981, 31300788) and the Hundred-Talent Program from the Chinese Academy of Sciences. The authors thank Wei Cui and Yuling Ma at the Institute of Metal Research, Chinese Academy of Sciences for assistance with sample preparation and microstructure characterization.

References

1. J. Leng, X. Lan, Y. Liu, and S. Du: Shape-memory polymers and their composites: Stimulus methods and applications. *Prog. Mater. Sci.* **56**, 1077–1135 (2011).
2. T. Xie: Tunable polymer multi-shape memory effect. *Nature* **464**, 267–270 (2010).
3. D. Zhao, T. van Leeuwen, J. Cheng, and B.L. Feringa: Dynamic control of chirality and self-assembly of double-stranded helicates with light. *Nat. Chem.* **9**, 250–256 (2017).
4. A.H. Gelebart, D.J. Mulder, G. Vantomme, A.P.H.J. Schenning, and D.J. Broer: A rewritable, reprogrammable, dual light-responsive polymer actuator. *Angew. Chem. Int. Ed.* **56**, 13436–13439 (2017).
5. M.Y. Razzaq, M. Behl, K. Kratz, and A. Lendlein: Multifunctional hybrid nanocomposites with magnetically controlled reversible shape-memory effect. *Adv. Mater.* **25**, 5730–5733 (2013).
6. J. Wang, L. Sun, M. Zou, W. Gao, C. Liu, L. Shang, Z. Gu, and Y. Zhao: Bioinspired shape-memory graphene film with tunable wettability. *Sci. Adv.* **3**, e1700004 (2017).
7. Y. Xiao, S. Zhou, L. Wang, and T. Gong: Electro-active shape memory properties of poly(ε-caprolactone)/functionalized multiwalled carbon nanotube nanocomposite. *ACS Appl. Mater. Inter.* **2**, 3506–3514 (2010).
8. H. Deng, Y. Dong, J.W. Su, C. Zhang, Y. Xie, C. Zhang, M.R. Maschmann, Y. Lin, and J. Lin: Bioinspired programmable polymer gel controlled by swellable guest medium. *ACS. Appl. Mater. Inter.* **9**, 30900–30908 (2017).
9. A.V. Salvekar, W. Huang, R. Xiao, Y.S. Wong, S.S. Venkatraman, K.H. Tay, and Z. Shen: Water-responsive shape recovery induced buckling in biodegradable photo-cross-linked poly(ethylene glycol) (PEG) hydrogel. *Acc. Chem. Res.* **50**, 141–150 (2017).
10. M. Ma, L. Guo, D.G. Anderson, and R. Langer: Bio-inspired polymer composite actuator and generator driven by water gradients. *Science* **339**, 186–189 (2013).
11. Z. Fang, Y. Kuang, P. Zhou, S. Ming, P. Zhu, Y. Liu, H. Ning, and G. Chen: Programmable shape recovery process of water-responsive shape-memory poly(vinyl alcohol) by wettability contrast strategy. *ACS. Appl. Mater. Inter.* **9**, 5495–5502 (2017).
12. X. Xiao and J. Hu: Animal hairs as water-stimulated shape memory materials: mechanism and structural networks in molecular assemblies. *Sci. Rep.* **6**, 26393 (2016).
13. Z. Liu, D. Jiao, and Z. Zhang: Remarkable shape memory effect of a natural biopolymer in aqueous environment. *Biomaterials* **65**, 13–21 (2015).
14. N.N. Ashton and R.J. Stewart: Self-recovering caddisfly silk: energy dissipating, Ca^{2+}-dependent, double dynamic network fibers. *Soft Matter* **11**, 1667–1676 (2015).
15. O. Emile, A.L. Floch, and F. Vollrath: Shape memory in spider draglines. *Nature* **440**, 621–621 (2006).
16. M. Baláž: Eggshell membrane biomaterial as a platform for applications in materials science. *Acta Biomater.* **10**, 3827–3843 (2014).
17. Q. Li, Y. Bai, T. Jin, S. Wang, W. Cui, I. Stanciulescu, R. Yang, H. Nie, L. Wang, and X. Zhang: Bioinspired engineering of poly(ethylene glycol) hydrogels and natural protein fibers for layered heart valve constructs. *ACS Appl. Mater. Inter.* **9**, 16524–16535 (2017).
18. X. Wang, Q. Li, Y. Yuan, B. Mei, R. Huang, Y. Tian, J. Sun, C. Cao, G. Lu, and G. Liang: New method for effectively and quantitatively labeling cysteine residues on chicken eggshell membrane. *Org. Biomol. Chem.* **10**, 8082–8086 (2012).
19. T. Nakano, N. Ikawa, and L. Ozimek: Chemical composition of chicken eggshell and shell membranes. *Poult. Sci.* **82**, 510–514 (2003).
20. K. Simkiss and C. Tyler: A histochemical study of the organic matrix of hen egg-shells. *Q. J. Microsc. Sci.* **98**, 19–28 (1957).
21. N. Li, L. Niu, Y. Qi, C.K.Y. Yiu, H. Ryou, D.D. Arola, J. Chen, D.H. Pashley, and F.R. Tay: Subtleties of biomineralisation revealed by manipulation of the eggshell membrane. *Biomaterials* **32**, 8743–8752 (2011).
22. V.K. Kodali, S.A. Gannon, S. Paramasivam, S. Raje, T. Polenova, and C. Thorpe: A novel disulfide-rich protein motif from avian eggshell membranes. *PLoS ONE* **6**, e18187 (2011).
23. H. Su, J. Han, N. Wang, Q. Dong, D. Zhang, and C. Zhang: In situ synthesis of lead sulfide nanoclusters on eggshell membrane fibers by an ambient bio-inspired technique. *Smart Mater. Struct.* **17**, 015045 (2008).
24. C. Li, H. Liao, X. Zhang, X. Yu, and M. Tong: Preparation of cationic modified collagen extracted from leather wastes and their application in dye flocculation. *J. Appl. Polym. Sci.* **134**, 45363 (2017).
25. H. Du and J. Zhang: Solvent induced shape recovery of shape memory polymer based on chemically cross-linked poly(vinyl alcohol). *Soft Matter* **6**, 3370–3376 (2010).
26. T. Yang, M. Chen, X. Hu, Z. Wang, J. Wang, and P.K. Dasgupta: Thiolated eggshell membranes sorb and speciate inorganic selenium. *Analyst* **136**, 83–89 (2011).
27. P.Y. Chen, J. Mckittrick, and M.A. Meyers: Biological materials: Functional adaptations and bioinspired designs. *Prog. Mater. Sci.* **57**, 1492–1704 (2012).
28. D.A. Carrino, J.E. Dennis, T.M. Wu, J.L. Arias, M.S. Fernandez, J.P. Rodriguez, D.J. Fink, A.H. Heuer, and A.L. Caplan: The avian eggshell extracellular matrix as a model for biomineralization. *Connect. Tissue Res.* **35**, 325–329 (1996).
29. F.G. Torres, O.P. Troncoso, F. Piaggio, and A. Hijar: Structure–property relationships of a biopolymer network: the eggshell membrane. *Acta Biomater.* **6**, 3687–3693 (2010).
30. C.A. Miles and A.J. Bailey: Thermally labile domains in the collagen molecule. *Micron* **32**, 325–332 (2001).

https://doi.org/10.1557/mrc.2018.100 Published online by Cambridge University Press